Ultrasonic-assisted Drilling of Laminated Aluminum 2024 Metal Matrix Composite Reinforced with SiC Nanoparticles: Experimental Investigation and Grey Relational Optimization

Farzad Pashmforoush
Faculty of Engineering, Department of Mechanical Engineering, University of Maragheh, P.O. Box 55136-553, Maragheh, Iran

Reza Farshbaf Zinati
Department of Mechanical Engineering, Branch of Tabriz, Azad University, Tabriz, Iran.

Asghar Dadashzadeh
Department of Mechanical Engineering, Branch of Tabriz, Azad University, Tabriz, Iran

Aluminum metal matrix composites are widely used in various engineering areas due to their excellent mechanical properties. However, due to their heterogeneous structure, efficient machining of these materials is still a challenging task. Therefore, in the present study the drilling performance of aluminium-copper alloy (Al 2024) reinforced with SiC nanoparticles was experimentally investigated, in the presence of ultrasonic vibration.In this regard, the influence of ultrasonic vibration, SiC weight fraction and drilling parameters was assessed on circularity error and drilling thrust force. Also, the optimization of process parameters was investigated using grey relational analysis. The performed calculations revealed that ultrasonic vibration, SiC content of 2 %wt, feed rate of 20 mm/min and spindle speed of 1400 rpm is the optimal parameters setting in the present study.

Keywords:*Aluminum metal matrix composites; ultrasonic-assisted drilling; grey relational analysis; thrust force; circularity error.*

1. INTRODUCTION

Metal matrix composites (MMCs) are advanced materials extensively used in different engineering areas such as automotive, aerospace and defense industries. In this regard, aluminium based MMCs possess superior properties over other composite materials such as high specific stiffness, low density, high thermal/electrical conductivity, high corrosion resistance and good reflective properties [1-4]. However, machining of these materials is still a challenging task because of their heterogeneous structure, which is due to the presence of a hard and brittle reinforcement phase (like SiC) in a ductile matrix (like Aluminium) [5]. Among various machining processes, drilling plays an important role in MMCs manufacturing. However, conventional drilling (CD) suffers from several problems such as high cutting temperature and force, poor surface integrity, high tool wear rate and wide dimensional/geometrical tolerances [6,7]. Hence, the application of advanced drilling processes such as ultrasonic assisted drilling (UAD) is of great importance for efficient machining of MMCs.

So far, numerous studies have been carried out toward the UAD of different materials. Pashmforoush et al. [8] studied the effect of ultrasonic vibration on drilling performance of natural filler reinforced composite materials. The obtained results revealed that ultrasonic vibration could considerably improve the geometrical tolerances and surface quality, which was due to the impact action of ultrasonic vibration and intermittent cutting process, leading to reduced friction coefficient, reduced cutting forces, improved material removal and better surface integrity.Cutting temperature and feed force was investigated by Pujana et al. [9] during drilling of Ti6Al4V. In accordance with the obtained results, UAD resulted in the higher cutting temperature, but lower feed force, in comparison to CD. Chang et al. [10] analyzed burr formation in UAD of aluminum 6061-T6. They developed an analytical model to estimate the drilling thrust force and burr height. Comparison with experimental results indicated the high accuracy of their analytical model in evaluating the burr height. Their analytical/experimental study demonstrated that the burr height can be considerably reduced in UAD by appropriate selection of drilling parameters and ultrasonic frequency. Yohei et al. [11] studied the effect of ultrasonic vibration on machining time of micro deep drilling process. The obtained results revealed that by applying ultrasonic vibrations, higher step feeds can be employed, which results in less machining time, without any undesirable effect on drill wear rate. Amini et al. [12] studied chip morphology and thrust force during UAD of Al2024-T6 alloy. An enhancement of 70% was achieved for the thrust force in UAD, as compared with CD. The chips produced in CD were reported to be continuous, while in UAD discontinuous smaller chips were formed. Similar research was done by Barani et al. [13] to study built-up edge and surface quality during UAD of Al2024-T6 alloy. It was reported that ultrasonic vibration resulted in less built-up edge and enhanced surface quality. Furthermore, in UAD less abrasion/ adhesion induced damage was observed in drill edges.

Received: January 2021, Accepted: March 2021
Correspondence to: Dr Reza Farshbaf Zinati
Department of Mechanical Engineering, Branch of Tabriz, Azad University, Tabriz, Iran
E-mail: reza.farshbaf.zinati@gmail.com
doi: 10.5937/fme2102401P

Reduction of friction coefficient, as a result of reciprocating tool motion, was reported to be the key reason enhancing the drilling efficiency. Liu et al. [14] compared the performance of various drilling methods such as CD, UAD, high-speed drilling and grinding drilling in drilling of composite laminates. They studied the influence of drilling parameters and drill geometry on tool life, thrust force and drilling induced delamination. The obtained results indicated the good performance of advanced drilling processes in comparison with ordinary conventional drilling. Phadnis et al. [15] performed a numerical-experimental study on drilling of carbon fiber reinforced plastic (CFRP) composite materials. It was reported that the drilling thrust force was reduced by the amount of ~30% in VD. Moreover, the obtained results of finite element simulation showed that in CD high stresses were generated in the vicinity of the drilled holes. Liu et al. [16] studied the feasibility of rotary ultrasonic elliptical machining in drilling of CFRP composite panels. Comparison of the obtained results of this drilling technique with those of CD revealed that surface roughness and cutting force were reduced, delamination at hole-exits was suppressed, and tool life and material removal rate were improved considerably. Krishnamorthy et al. [17] investigated optimization of drilling parameters during CFRP drilling. Based on the grey fuzzy logic, the optimization of output responses (torque, thrust force, eccentricity of the holes and delamination) was carried out and the optimum combination of drilling parameters was obtained. The obtained results showed that high spindle rotational speeds, low feed rates and low point angles of drill resulted in the best surface quality. Ding et al. [18] studied the performance of rotary ultrasonic machining (RUM) during drilling of CFR silicon carbide (C/SiC) composites. It was reported that surface roughness and hole-quality were effectively improved in RUM. Also, less brittle fracture and shallower pits (initiating from carbon fibers fracture) were observed in RUM. Zou et al. [19] investigated the machining efficiency of C/SiC composites during CD process. It was reported that the predominant material removal mechanisms were matrix cracking, fiber breakage and fiber/matrix debonding. Baraheni et al. [20] performed parametric study for delamination analysis of glass fiber reinforced polymer composites during RUM process. They investigated the effect of drilling parameters, thermal fatigue conditions and addition of multi-walled carbon nanotubes on drilling induced delamination. It was demonstrated that by increase of the cutting velocity, delamination quality can be well optimized. Also, it was seen that addition of the appropriate content of carbon nanotubes enhances the delamination state; while, thermal fatigue condition leads to delamination deterioration. Sekaran et al. [21] made up natural fiber reinforced composites via hand layup method. Epoxy resin was used as matrix, and Aloe Vera and sisal were used as reinforcement. Performing CD tests, they studied the effect of drilling parameters on surface quality and delamination. In accordance with the obtained results, sisal showed less surface roughness and delamination at high spindle speeds and high feed rates, in comparison to Aloe Vera.

Wang et al. [22] studied the drilling operation of natural fiber (hemp) reinforced polymer composites. The results revealed that for different ranges of drilling parameters, UAD was more effective than CD, particularly for heterogeneous composite materials. UAD offered lower machining forces and energies, which led to enhanced surface integrity, better hole quality, less burr formation and reduced fiber pull-out damage.

Soni et al. [23]investigated the mechanical properties and machinability of Al7075/SiC/h-BN hybrid nanocomposite. According to the obtained results, the reinforced nanoscale h-BN particles acted as a solid lubricant during the dry machining, resulting in the better surface quality of the machined surface. The lowest surface roughness and cutting force were observed during the minimum quantity lubrication (MQL) machining of nanocomposites, which was related to the combined lubrication layer mechanism achieved by reinforced h-BN nanoparticles and MQL.

Elango et al. [24] investigated the optimization of machining parameters of Al/SiC/Gr hybrid metal matrix composites. According to the results of analysis of variance (ANOVA), feed rate was the most significant parameter affecting the surface roughness, followed by cutting speed and depth of cut.

Waleed et al. [25] studied the effect of drilling parameters in thermal drilling of the metal matrix composites (Copper Silicon carbide). The obtained results revealed that torque and thrust force increased with increase of feed rate, decrease of spindle speed and increase of the drill conical angle.

In accordance with the above mentioned literature, the majority of the studies performed in the field of UAD have been focused on conventional alloys and polymer matrix composite materials. There are limited studies toward the application of UAD for metal matrix composites [26-28]. As mentioned earlier, aluminium metal matrix composites possess several advantageous over conventional materials; however, their machining is much more difficult and challenging. Therefore, the machinability analysis of these materials is of great significance for a variety of industrial applications.

So, in this research the drilling performance of aluminium based MMC reinforced with SiC nanoparticles (Al 2024/SiC) was experimentally evaluated. By performing the drilling tests, the effect of drilling parameters, SiC weight fraction and ultrasonic vibration was assessed on thrust force and geometrical tolerances (the holes' circularity). Also, the optimization of process parameters was investigated using grey relational analysis. The multi-objective optimization problem was converted to single-objective problem, and then based on the grey relational grade values, the optimal parameters setting was achieved.

2. EXPERIMENTAL SET-UP

The experimental set-up is demonstrated in Fig. 1. The set-up consists of a CNC vertical milling machine (DECKEL model), vibration unit and dynamometer.

The vibration unit includes ultrasonic generator, transducer and horn. The ultrasonic generator utilized in this study was an MPI model with frequency range of 18-23

KHz, 3000 W power and amplitude range of 1-30 μm. The transducer applied was piezoelectric type (MPI model) with 1200 W power, as shown in Fig. 2. Due to the rotation of the transducer (in spite of feed movement and ultrasonic oscillations), it was mounted on a rotating frame. The horn, as employed for amplitude amplification, was fabricated from aluminium 7075, which has superior acoustic properties, high stiffness and low density.

Figure 1. Experimental set-up of ultrasonic-assisted drilling process

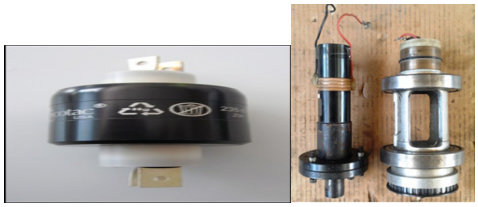

(a) **(b)**

Figure 2. (a) Ultrasonic transducer with rotating frame; (b) Slipping ring

The horn was designed in a conical shape with outer diameter of 32 mm, as shown in Fig.3. The angle and length of the horn was estimated through the modal analysis (based on finite element method), in a way that the resonance frequency of the horn conforms the longitudinal resonance frequency of the transducer. Based on the trial and error method, the horn geometry (angle and length) was calculated, resulting in the resonance frequency of 20117 Hz, lying in the resonance frequency range of the applied transducer.

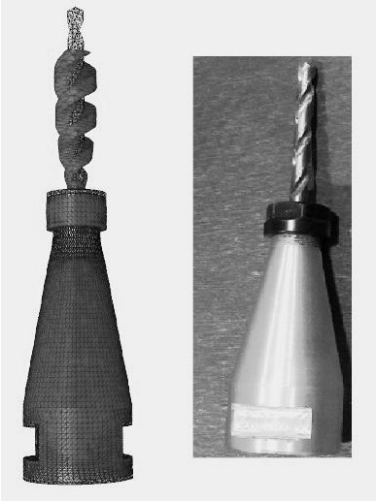

Figure 3. Designed and fabricated horn

Thrust force measurement was done by a KISTLER 9255B dynamometer, as illustrated in Fig. 4a.

The quality of the holes surfaces was assessed using visual measuring machine (VMM), as depicted in Fig. 4b. The VMM employed in this study has a magnification of 220X and resolution of 1 μm.

(a)

(b)

Figure 4. Devices used for the measurement of: (a) thrust force (KISTLER 9255B dynamometer); (b) circularity error (visual measuring machine).

The test specimens were laminated metal matrix composites made of Al-Cu alloy (Al 2024), as the matrix; and SiC nanoparticles, as reinforcement. The chemical composition of Al 2024 is summarized in Table 1 [29].

Table 1. Chemical composition of Al 2024 [23].

Composition	Cu	Mg	Mn	Fe	Si	Zn	Ti	Al
Wt (%)	4.82	1.5	0.657	0.178	0.0426	0.137	0.0169	bal

The nanoparticles were beta-phase SiC with diameter of 40-60 nm and purity of 99%. By performing preliminary harness and strength tests, the optimum weight fraction of these nanoparticles was obtained as 1-2%. The composite specimens were fabricated through accumulative channel compressed bonding (ACCB) method. The process was performed by a hydraulic press, by applying 240 bar pressure under 300^0C, leading to thickness reduction of 53-62%. The geometrical specifications of these specimens are listed in Table 2.

Table 2. Geometrical specifications of fabricated metal matrix composites.

Group	No. of layers	SiC content (%wt)	Initial length (mm)	Initial thickness (mm)	Final length (mm)	Final thickness (mm)	Strain (%)
1	7	2	100	7	120.73	3.25	53.57
2	7	1	100	6.69	120.58	2.50	62.63

To evaluate the mechanical properties of the fabricated composites, universal tensile tests and Vickers hardness tests were carried out. The obtained results, as summarized in Table 3, showed that specimens with 2 %wt of SiC nanoparticles possessed highest yield strength and ultimate tensile strength.

Table 3. Obtained results of universal tensile test.

Group	SiC content (%wt)	Yield strength (MPa)	Ultimate tensile strength (MPa)	Elongation percentage (%)
1	1	92	195	19
2	2	115	222	14

The cutting tool used for drilling tests was a twist HSS drill coated by cobalt, with pitch of 28 mm, diameter of 5 mm, point angle of 120°, helix length of 86 mm and helix angle of 28°. The cutting tool and the drilled specimens are shown in Fig. 5a and b, respectively.

(a) (b)

Figure 5. (a) The cutting tool (twist HSS drill coated by cobalt) and(b) Drilled specimens.

The process parameters under were drilling type (conventional or vibration assisted), spindle rotational speed, feed rate (varying in three levels) and SiC weight fraction (varying in two levels). The output responses were holes' circularity error and thrust force. The experimental tests were planned based on the full factorial design method, hence, 36 run tests were planned; 18 for vibration drilling and 18 for conventional drilling. The process parameters and their levels are listed in Table 4.

Table 4. The levels of process parameters.

Parameters	Levels		
	Low	Medium	High
Spindle rotational speed (rpm)	1100	1400	1700
Feed rate (mm/min)	20	60	100
SiC content (%wt)	1	-	2

3. GREY RELATIONAL ANALYSIS

Most of the engineering optimization problems are involved with multiple objective functions, in which, there isn't a unique solution that simultaneously optimizes all objectives. A well-organized technique for solving such multi-objective problems is to convert them to a single-objective optimization. In this respect, grey relational analysis is a promisingmethod thatnowadays is being extensively used in several engineering applications [30-32].

The first step of grey relational analysis is data preprocessing, in which the existing data are transformed to single scale, for the purpose of better comparison. This is done by normalizing the data in the range between 0 and 1. This process, called as grey relational generating, is required when the range or the unit of the output responses (i.e. thrust force and cylindricity error) is different from each other. Depending on the optimization criterion, there are three methods for data normalization. In the case of "larger-the-better" characteristics, data normalization is done by (1) [32]:

$$x_i(k) = \frac{y_i(k) - \min y_i(k)}{\max y_i(k) - \min y_i(k)} \tag{1}$$

where, $x_i(k)$ is the normalized data,i denotes the experiment number, k is the number of factors, and max $y_i(k)$ and min $y_i(k)$ are the highest and the lowest values of the k^{th} response, respectively.

In the case of the "smaller-the-better" characteristics, data normalization is done according to (2) [32]:

$$x_i(k) = \frac{\max y_i(k) - y_i(k)}{\max y_i(k) - \min y_i(k)} \tag{2}$$

In the case of the "nominal-the-better" characteristics, data normalization is done by (3) [32]:

$$x_i(k) = 1 - \frac{|\, y_i(k) - y^* \,|}{\max\{\max y_i(k) - y^*, y^* - \min y_i(k)\}} \tag{3}$$

where, y^* is the target ideal value of the output response.

After the data normalization, the grey relational coefficient (GRC) is calculated by (4) [32]:

$$\xi_i(k) = \frac{\Delta_{\min} + \lambda\Delta_{\max}}{\Delta_{0i}(k) + \lambda\Delta_{\max}} \quad \Delta_{0i}(k) = \left\| x_0(k) - x_i(k) \right\| \tag{4}$$

where, Δ is the absolute difference, Δmax and Δmin are respectively the maximum and the minimum values of the absolute difference, and λ is the identification coefficient, lying in the interval between 0 and 1 (usually is equal to 0.5).

Finally, by averaging the calculated GRCs, the grey relational grade (GRG) is calculated, which is employed to measure the correlation between the ideal and actual data. The higher is the grey relational grade; the closer is the process parameter to the optimal value. GRG is calculated by (5):

$$\gamma_i = \frac{1}{n}\sum_{k=1}^{n} w_i \xi_i(k), \ \sum_{k=1}^{n} w_i = 1 \tag{5}$$

where, γ represents the grey relational grade value, n is the number of responses and w is the importance weight of output responses. In this study the output responses (i.e. thrust force and circularity error) have equal importance and hence have equal weights.

Now, by means of the calculated grey relational grade, the multi-objective optimization problem is transformed to the single-objective optimization.

4. RESULTS AND DISCUSSION

4.1 Thrust force analysis

The drilling tests were carried out with and without ultrasonic vibration and the thrust force was measured

by KISTLER 9255B dynamometer. In this respect, the vibration was exerted to the cutting tool (drill) in the feed direction and the trust force of UAD was calculated and compared with that of the conventional drilling. The obtained results, as listed in Table 5, show that the thrust force is varying in the range between 26 N and 200 N. Its minimum value is achieved at spindle speed of 1400 rpm, feed rate of 20 mm/min and SiC content of 1 %wt; in the case of UAD. The influence of ultrasonic vibration, SiC content and drilling parameters on thrust force is discussed by detail in the following sections.

4.1.1 Influence of ultrasonic vibration on the thrust force

The interactive effect of ultrasonic vibration and process parameters is illustrated in Fig. 6.

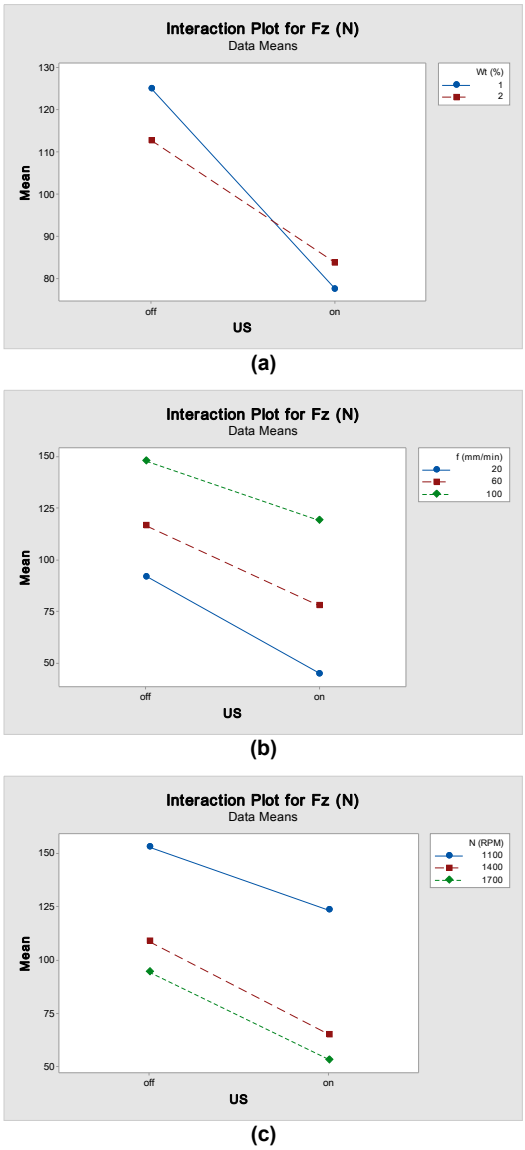

Figure 6. Interactive effect of ultrasonic (US) vibration and: (a) SiC content, (b) feed rate and (c) spindle speed; on thrust force.

As shown, in all cases the thrust force of UAD is less than that of CD. The best improvement is 69%, achieved at spindle speed of 1400 rpm, feed rate of 20 mm/min and SiC content of 1 %wt. The reduction of the thrust force in UAD can be related to intermittent cutting process caused by ultrasonic vibration which results in the frequent separation of the chip and the drill rake face; leading to the reduction of the interface friction between the chip and the tool, and accordingly reduction of the thrust force [8]. The second factor affecting the thrust force is due to the change of the effective rake angle of the drill. In UAD, during the downward movement of the drill (i.e. the first step of ultrasonic oscillation), the oscillation speed is added up with the feed speed, giving large negative angle, which leads to the reduction of the thrust force [8]. In addition, the impact action of the ultrasonic vibration eases chip breakage, which enhances the material removal process and reduces the thrust force [13].

4.1.2 Effect of SiC content on thrust force

The interactive effect of SiC content and drilling parameters is depicted in Fig. 7.

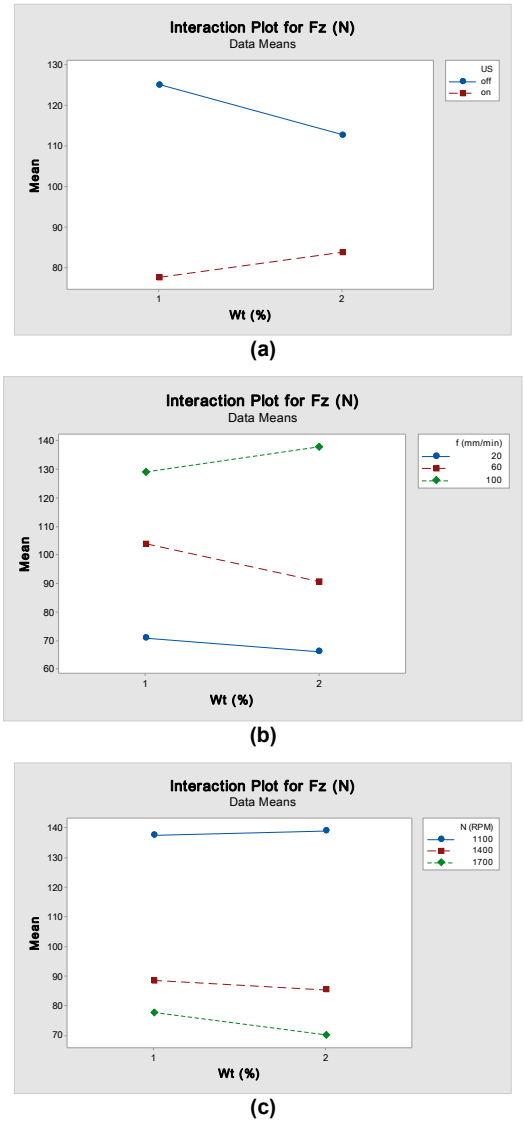

Figure 7. Interactive effect of SiC content and: (a) ultrasonic (US) vibration, (b) feed rate and (c) spindle speed; on thrust force.

It is evident that in contrast to CD, in UAD by increase of SiC weight fraction, the thrust force decreases. In UAD, the material removal takes place due to the impact forces induced by ultrasonic vibration. Hence,

fracture toughness of the composite specimens plays a significant role in chip formation process. By adding SiC reinforcement to Al matrix, the fracture toughness of the specimens decreases [33], which facilitates the chip formation and consequently reduces the required thrust force. However, in CD by increase of SiC weight fraction, the thrust force increases, owing to the different material removal characteristic, in which, material removal doesn't take place by impact action. Hence, material flow strength (instead of fracture toughness) is the predominant material property that affects the thrust force. Since, by increase of SiC content, the material flow strength increases [33], the required cutting force increases. The variation of thrust force with drilling time is illustrated in Fig. 8 for SiC content of 1%wt and 2%wt.

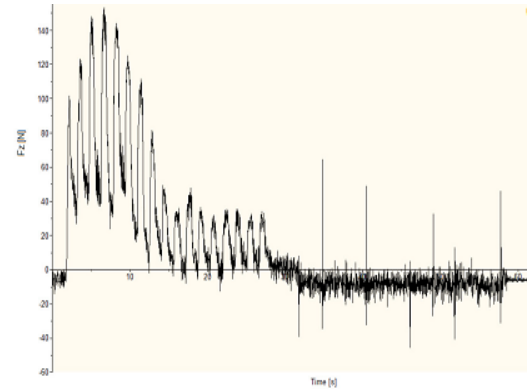

(a)

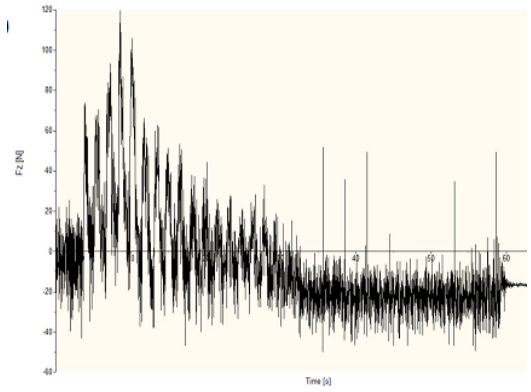

(b)

Figure 8. Variation of thrust force with drilling time in UAD for SiC content of: (a) 1%wt and (b) 2 %wt. (spindle speed= 1100 rpm and feed rate= 20 mm/min).

4.1.3 Effect of drilling parameters on thrust force

The interactive effect of spindle speed and feed rate is shown in Fig. 9.

As illustrated, by increase of feed rate, the thrust force increases, owing to the increased chip cross section. In each rotation of the drill, by increase of the chip cross section, more material endures plastic deformation and accordingly more material is involved in the material removal process, leading to the increased thrust force. Moreover, by increase of feed rate, the strain rate increases, which in turn increases the material flow strength, and accordingly increases the thrust force. The relationship between the strain rate and the flow stress can be explained according to the Johnson-Cook plasticity model [34], as given by (6); and the relationship between feed rate and strain rate is explained by (7):

$$\bar{\sigma}(MPa) = (A + B\varepsilon^{n})(1 + C\ln\frac{\dot{\varepsilon}}{\dot{\varepsilon}_0})(1 - (\frac{T - T_{room}}{T_{melt} - T_{room}})^{m}) \quad (6)$$

$$\dot{\varepsilon} = \frac{f}{t} + \frac{2\pi a\upsilon}{2a} \quad (7)$$

where, σ is the flow stress, ε is plastic strain, $\acute{\varepsilon}$ is the plastic strain rate, T is temperature, T_{melt} is the melt temperature and T_{room} is the reference temperature. A, B, C, n and m are material constants. $\acute{\varepsilon}$ is the strain rate, f is feed rate and t is the workpiece thickness. υ and a are vibration frequency and amplitude, respectively.

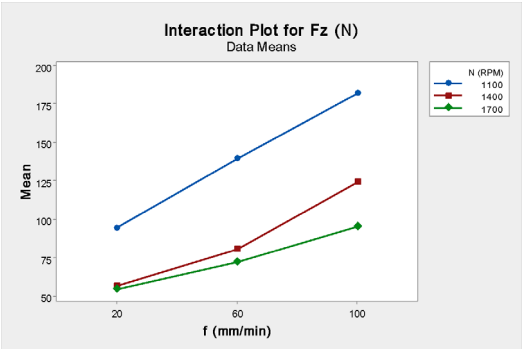

Figure 9. Interactive effect of spindle speed and feed rate on thrust force.

As demonstrated, in UAD the strain rate consists of two main components; one due to the feed rate (in materials' thickness direction); and one due to the vibration speed (in amplitude direction).

Looking back to the obtained results, it is evident that by increase of spindle speed, the thrust force is reduced, which is related to the thermal softening phenomenon. As the rotational speed increases, the drilling temperature also increases, and accordingly the material strength decreases, resulting in reduced thrust force [35]. Also, increased spindle rotational speed leads to the chips segmentation, which reduces the chips plastic deformation and consequently reduces the thrust force. In addition, by increase of spindle speed, the friction coefficient decreases (provided that built-up edge (BUE) doesn't form), and hence the thrust force decreases. In low cutting speeds, due to the BUE formation, thrust forces increase with increase of the spindle speed. However, in higher speeds, BUE formation doesn't occur and consequently the thrust force shows decreasing tendency with increase of spindle speed, due to the reduction of friction coefficient.

4.2 Circularity error analysis

In drilling process, the circularity error (CE) is caused by plastic deformation of the drilled holes. Plastic deformation itself is dependent on the thrust force. Therefore, the interactive influence of ultrasonic vibration, SiC content and drilling parameters on the thrust force determines the severity of the holes' plastic deformation and accordingly the circularity error. Also, the influence of process parameters on burr formation is another issue

affecting the circularity error. In the following sections, these effects are discussed in detail.

4.2.1 Effect of ultrasonic vibration on circularity error

The interactive effect of ultrasonic vibration and drilling parameters is illustrated in Fig. 10. For all values of spindle speeds, the circularity error of UAD is less than that of CD, due to the reduced thrust force (as discussed in section 4.1.1), and consequently reduced plastic deformation of the drilled holes. Unlike the influence of ultrasonic vibration at all values of spindle speed, its influence at different feed rates is completely different. At feed rates of 60 and 100 mm/min, the circularity error of UAD is less than that of CD; in contrast to feed rate of 20 mm/min.

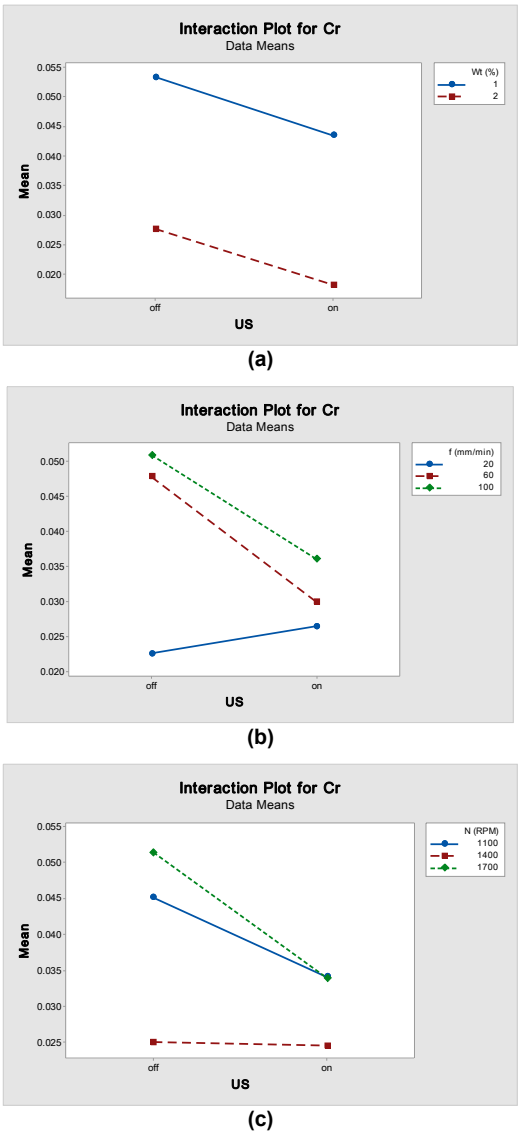

Figure 10. Interactive effect of ultrasonic (US) vibration and: (a) SiC content, (b) feed rate and (c) spindle speed; on circularity error.

This phenomenon relates to the drill slipping and skidding, which usually occurs at lower feed rates. Also, it is reported that at lower thrust forces, the drill slipping gets much more severe, especially at hole entrance [36,37]. Therefore, the circularity error of UAD is more than that of CD. However, at higher feed rates, the drill slipping doesn't occur, and hence, the reduced plastic deformation of UAD (as a result of reduced thrust force) reduces the circularity error. The other factor affecting the circularity error is burr formation. According to the VMM images (as shown in Figs. 11 and 12), in UAD, less burr formation can be observed at both hole entrance and end surfaces. So, improved surface quality with lower circularity error is obtained in the case of UAD.

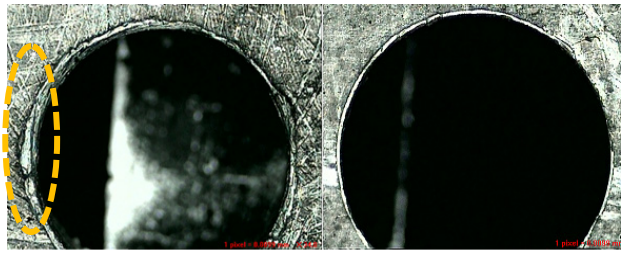

(a) (b)

Figure 11. VMM images of holes "entrance" surface; (a) CD and (b) UAD. (SiC content= 1 %wt; feed rate= 20 mm/min; spindle speed= 1400 RPM)

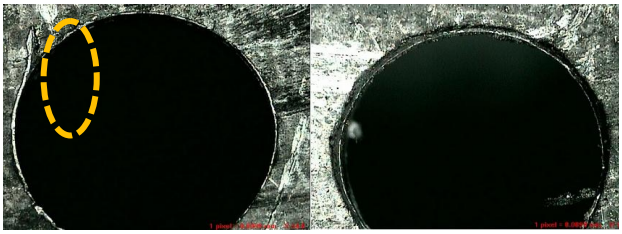

(a) (b)

Figure 12. VMM images of holes "end" surface; (a) CD and (b) UAD. (SiC content= 1 %wt; feed rate= 20 mm/min; spindle speed= 1400 RPM)

4.2.2 Effect of SiC content on circularity error

The interactive effect of SiC content and drilling parameters is illustrated in Fig. 13.

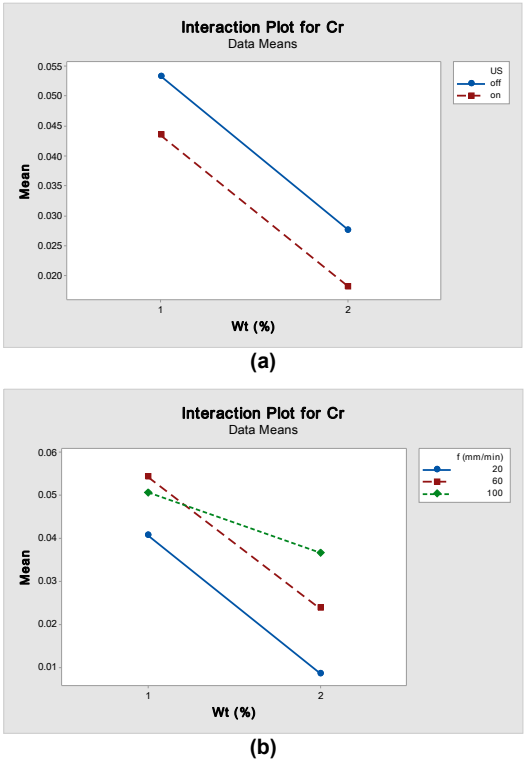

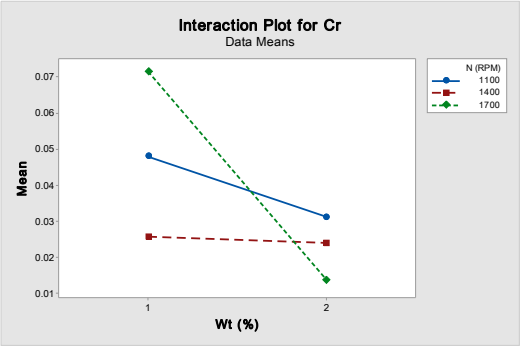

(c)

Figure 13. Interactive effect of SiC content and: (a) ultrasonic (US) vibration, (b) feed rate and (c) spindle speed; on circularity error.

It is evident that for all values of process parameters, the circularity error decreases with increase of the SiC weight fraction. This is due to the strengthening effect of SiC, which increases the material resistance against the plastic deformation, leading to less plastic deformation in holes' entrance and exit sides, and consequently resulting in less circularity error. Also, due to the brittle nature of SiC reinforcement, increase of its weight fraction leads to discontinuous chip formation, which in turn causes less burr formation. The VMM images of holes' entrance and end surfaces (as shown in Figs. 14 and 15) reveal that by increasing the SiC content, less plastics deformation and less burr formation occurs, resulting in reduced circularity error.

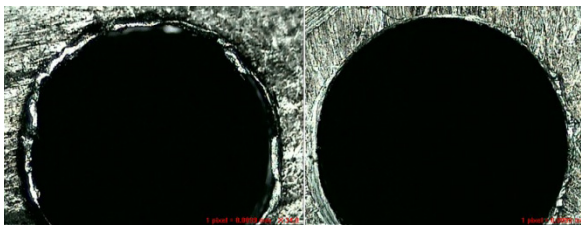

(a) (b)

Figure 14. VMM images of holes "entrance" surface in CD for; (a) 1 %wtSiC and (b) 2 %wtSiC.

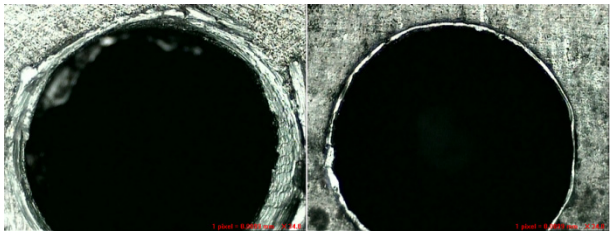

(a) (b)

Figure 15. VMM images of holes' end surface in CD for; (a) 1 %wtSiC and (b) 2 %wtSiC.

4.2.3 Effect of drilling parameters on circularity error

The interactive effect of feed rate and spindle speed is depicted in Fig. 16.

As shown, by increase of the feed rate, the circularity error increases, due to the increase of the thrust force. As mentioned earlier, increase of the feed rate results in increase of the chip cross section, leading to the increased thrust force and higher circularity error. In addition, increase of the chip thickness leads to more burr formation in holes' surfaces, and accordingly leads to more circularity error. This fact is well illustrated in Figs. 17 and 18, which demonstrate the VMM images taken at drill entrance and end sides, for the feed rates of 20 and 100 mm/min.

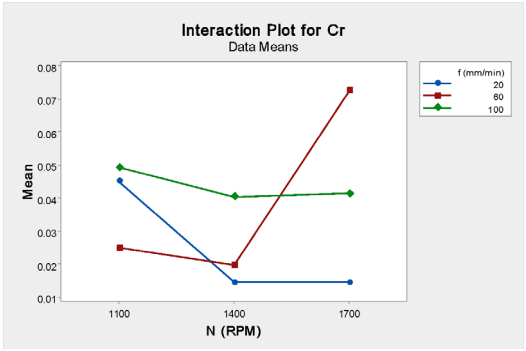

Figure 16. Interactive effect of spindle speed and feed rate on circularity error.

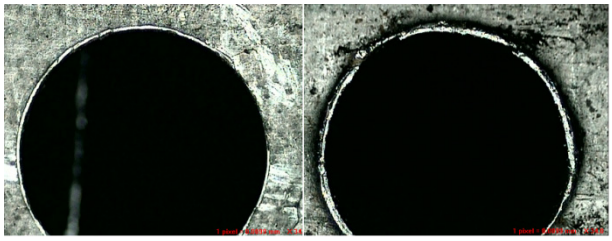

(a) (b)

Figure 17.VMM images of holes "entrance" surface in CD at feed rates of: a) 20 mm/min, and b) 100 mm/min.

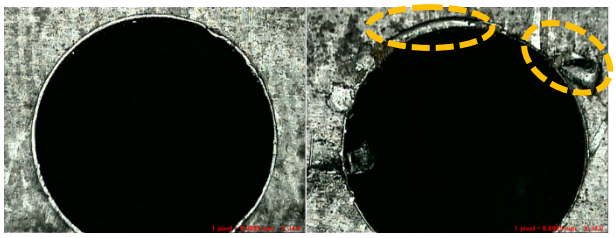

(a) (b)

Figure 18.VMM images of holes' end surface in CD at feed rates of: a) 20 mm/min, and b) 100 mm/min.

The effect of spindle rotational speed on circularity error is somewhat complicated. At feed rates of 20 and 100 mm/min, increase of the spindle speed leads to the decrease of the circularity error; while, at feed rate of 60 mm/min, by increase of the spindle speed, the circularity error firstly decreases, but then increases. This phenomenon depends on the combined effect of the thrust force and the cutting temperature. At feed rate of 100 mm/min, the heat transfer rate is high, and, hence, the role of the cutting force on plastic deformation is more dominant than that of the heat generation (cutting temperature). So, by increase of the spindle speed, since the cutting forces decrease, less plastic deformation occurs, and consequently circularity error is reduced. While, at feed rate of 60 mm/min, the heat transfer rate isn't very much, and hence, the role of heat generation on plastic deformation is more dominant than that of the cutting force. Therefore, by increase of spindle speed, more heat is generated and more plastic deformation occurs, leading to the increased circularity error. At feed rate of 20 mm/min, since the cutting

temperature isn't very high, again, the cutting force determines the severity of the plastic deformation. So, by increase of the spindle speed, the circularity error is reduced, due to the decreased cutting forces. The effect of spindle speed on burr formation is illustrated by VMM images, as shown in Figs. 19 and 20.

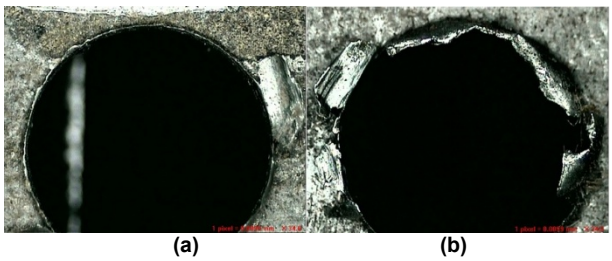

(a) (b)

Figure 19. VMM images of holes "entrance" surface in CD at spindle speeds of: a) 1100 rpm, and b) 1700 rpm.

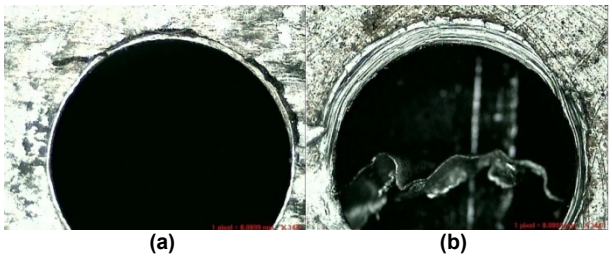

(a) (b)

Figure 20. VMM images of holes' end surface in CD at spindle speeds of: a) 1100 rpm, and b) 1700 rpm.

4.3 Optimization of process parameters

The optimization problem of the present study is involved with two output responses, i.e. the thrust force and the circularity error. Hence, as mentioned in section 3, the problem should be converted to single objective optimization through grey relational analysis. For this purpose, first, the data pre-processing was performed by normalizing the data set in the range between 0 and 1. Since, the objective functions are based on the minimization of both thrust force and circularity error, the data normalization was performed through "smaller-the-better" characteristic, using (2).Then, the grey relational coefficients (GRCs) were calculated using the (4). Finally, the grey relational grade (GRG) was calculated by averaging the GRCs. The obtained results of grey relational analysis are summarized in Table 6.

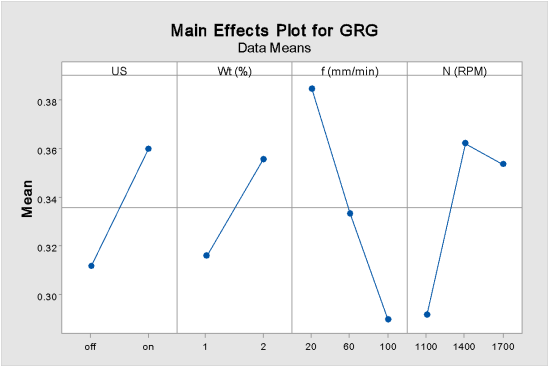

Figure 21. Interactive effect of process parameters on grey relational grade.

Table 5 Summary of the measured thrust force and circularity error in CD and UAD.

Run order	Drilling type	Feed rate (mm/min)	Spindle speed (rpm)	SiC content (%wt)	Thrust force (N)	Circularity error (mm)
1	UAD	20	1100	1	72	0.0608
2	UAD	20	1400	1	26	0.0370
3	UAD	20	1700	1	34	0.0324
4	UAD	60	1100	1	123	0.0384
5	UAD	60	1400	1	70	0.0076
6	UAD	60	1700	1	47	0.1050
7	UAD	100	1100	1	166	0.0464
8	UAD	100	1400	1	83	0.0294
9	UAD	100	1700	1	77	0.0275
10	UAD	20	1100	2	72	0.0097
11	UAD	20	1400	2	38	0.0084
12	UAD	20	1700	2	27	0.0033
13	UAD	60	1100	2	128	0.0090
14	UAD	60	1400	2	44	0.0059
15	UAD	60	1700	2	55	0.0137
16	UAD	100	1100	2	181	0.0331
17	UAD	100	1400	2	129	0.0584
18	UAD	100	1700	2	79	0.0216
19	CD	20	1100	1	124	0.0933
20	CD	20	1400	1	86	0.0490
21	CD	20	1700	1	83	0.0800
22	CD	60	1100	1	161	0.0185
23	CD	60	1400	1	116	0.0650
24	CD	60	1700	1	106	0.1491
25	CD	100	1100	1	180	0.0237
26	CD	100	1400	1	150	0.0682
27	CD	100	1700	1	119	0.1077
28	CD	20	1100	2	109	0.0870
29	CD	20	1400	2	76	0.0071
30	CD	20	1700	2	74	0.0137
31	CD	60	1100	2	145	0.0331

32	CD	60	1400	2	91	0.0584
33	CD	60	1700	2	80	0.0216
34	CD	100	1100	2	200	0.0933
35	CD	100	1400	2	134	0.0049
36	CD	100	1700	2	105	0.0080

Table 6. The obtained results of grey relational analysis.

No.	Normalized data		Δ_{0i}		GRC		GRG
	Thrust force	Circularity error	Thrust force	Circularity error	Thrust force	Circularity error	
1	0.7356	0.5562	0.2644	0.4438	0.6541	0.5298	0.296
2	1	0.7689	0	0.2311	1	0.6839	0.421
3	0.954	0.8004	0.046	0.1996	0.9158	0.7147	0.4076
4	0.4425	0.7593	0.5575	0.2407	0.4728	0.675	0.287
5	0.7471	0.9705	0.2529	0.0295	0.6641	0.9443	0.4021
6	0.8793	0.3025	0.1207	0.6975	0.8056	0.4175	0.3058
7	0.1954	0.7044	0.8046	0.2956	0.3833	0.6284	0.2529
8	0.6724	0.821	0.3276	0.179	0.6042	0.7364	0.3351
9	0.7069	0.834	0.2931	0.166	0.6304	0.7508	0.3453
10	0.7356	0.9561	0.2644	0.0439	0.6541	0.9193	0.3934
11	0.931	0.965	0.069	0.035	0.8788	0.9346	0.4534
12	0.9943	1	0.0057	0	0.9886	1	0.4972
13	0.4138	0.9609	0.5862	0.0391	0.4603	0.9275	0.3469
14	0.8966	0.9822	0.1034	0.0178	0.8286	0.9656	0.4485
15	0.8333	0.9287	0.1667	0.0713	0.75	0.8752	0.4063
16	0.1092	0.7956	0.8908	0.2044	0.3595	0.7098	0.2673
17	0.408	0.6221	0.592	0.3779	0.4579	0.5695	0.2569
18	0.6954	0.8745	0.3046	0.1255	0.6214	0.7993	0.3552
19	0.4368	0.3827	0.5632	0.6173	0.4703	0.4475	0.2294
20	0.6552	0.989	0.3448	0.011	0.5918	0.9785	0.3926
21	0.6724	0.9678	0.3276	0.0322	0.6042	0.9394	0.3859
22	0.2241	0.8957	0.7759	0.1043	0.3919	0.8275	0.3048
23	0.4828	0.9781	0.5172	0.0219	0.4915	0.958	0.3624
24	0.5402	0	0.4598	1	0.521	0.3333	0.2136
25	0.1149	0.8601	0.8851	0.1399	0.361	0.7814	0.2856
26	0.2874	0.5549	0.7126	0.4451	0.4123	0.529	0.2353
27	0.4655	0.284	0.5345	0.716	0.4833	0.4112	0.2236
28	0.523	0.963	0.477	0.037	0.5118	0.931	0.3607
29	0.7126	0.9739	0.2874	0.0261	0.635	0.9505	0.3964
30	0.7241	0.9287	0.2759	0.0713	0.6444	0.8752	0.3799
31	0.3161	0.7956	0.6839	0.2044	0.4223	0.7098	0.283
32	0.6264	0.6221	0.3736	0.3779	0.5724	0.5695	0.2855
33	0.6897	0.8745	0.3103	0.1255	0.617	0.7993	0.3541
34	0	0.3827	1	0.6173	0.3333	0.4475	0.1952
35	0.3793	0.989	0.6207	0.011	0.4462	0.9785	0.3562
36	0.546	0.9678	0.454	0.0322	0.5241	0.9394	0.3659

The higher is the GRG; the closer is the process parameter to the optimum value. Hence, the optimal parameters setting for minimizing the thrust force and the circularity error is the one with the maximum GRG value. As illustrated in Fig. 21 and Table 6; ultrasonic vibration, 2 %wt of SiC nanoparticles, feed rate of 20 mm/min and spindle speed of 1400 rpm is the optimal parameters setting in the present study.

5. CONCLUSION

In this study, the drilling performance of aluminium-copper alloy (Al 2024) reinforced with SiC nanoparticles was experimentally evaluated. In this respect, first, the metal matrix composite specimens were fabricated through the accumulative channel compressed bonding technique; and then the drilling tests were carried out, with and without ultrasonic vibration. The effect of drilling parameters, SiC weight fraction and ultrasonic vibration was assessed for geometrical tolerances (circularity error) and thrust force. Also, the optimization of process parameters was performed based on the grey relational analysis. The following conclusions can be drawn from the present research:

- By applying ultrasonic vibration, the thrust force was considerably reduced. The best improvement was 69%, achieved at feed rate of 20 mm/min, spindle speed of 1400 rpm and SiC content of 1 %wt.
- The influence of ultrasonic vibration on thrust force is related to the impact action of ultrasonic vibration and intermittent cutting process, which leads to the reduced friction coefficient, increased effective rake angle, improved material removal, and consequently reduced cutting forces.
- In UAD, by increase of SiC content, the thrust force decreased; unlike CD. This was attributed to different material removal mechanism involved with each process. In UAD, due to the impact

forces of vibrations, fracture toughness plays significant role in material removal process; while in CD (due to the lack of the impact forces), flow strength is the predominant material property affecting the material removal.

- For all values of spindle speeds, the circularity error of UAD was less than that of CD, due to the reduced thrust force and consequently reduced plastic deformation of the drilled holes. However, the effect of ultrasonic vibration at different feed rates was completely different, which was related to the drill slipping and skidding, which usually occurs at lower feed rates.
- Circularity error showed decreasing tendency with increase of SiC weight fraction. This is due to the strengthening effect of SiC, which increases the material resistance against plastic deformation in the holes' entrance and exit sides, and consequently results in less circularity error. Also, due to the brittle nature of SiC reinforcement, increase of its weight fraction leads to discontinuous chip formation, which in turn causes less burr formation.
- By increase of feed rate, the circularity error increased, due to the increase of the thrust force. However, the influence of spindle speed on circularity error was somewhat complicated; depending on the combined effect of the thrust force and the cutting temperature.
- Based on the grey relational analysis and calculated GRG values; ultrasonic vibration, 2 %wt of SiC nanoparticles, feed rate of 20 mm/min and spindle speed of 1400 rpm was the optimal parameters setting.
- Finally, the investigation of the effect of other machining processes such as milling, electro-discharge machining, laser beam machining, etc. on the laminated nano-compositesis suggested for the future works. Also, the machinability analysis of *hybrid*nano-composites can be investigated in the future works.

REFERENCES

[1] Kim, E.H. et al.: Fabrication and mechanical properties of metal matrix composite with homogeneously dispersed ceramic particles, Ceramics International, Vol. 39, No. 6: pp. 6503-6508, 2013.

[2] Beaumont P.W.R., Soutis C. Hodzic A. (Editors): Structural integrity and durability of advanced composites: Innovative modelling methods and intelligent design, Woodhead Publishing - Elsevier, Cambridge, 2015.

[3] Zweben C.H. and Beaumont P.W.R. (Editors): Comprehensive Composite Materials II, 2nd Edition, Elsevier Ltd., Amsterdam, 2018.

[4] Jawaid, M., Thariq, M. (Editors): Handbook Sustainable Composites for Aerospace Applications, Woodhead Publishing - Elsevier, Cambridge, 2018.

[5] Jain, P.K, Bareder, P.,Soni,S.C, Development of Silicon Carbide Particle Reinforced Aluminium 6101 Metal Matrix Composite Using Two-Step Stir Casting, Materials Today: Proceedings, Vol. 18, No. 7: pp. 3521-3525, 2019.

[6] Shyha, I.S., Soo, S.L., Aspinwall, D., Bradley, S., Effect of laminate configuration and feed rate on cutting performance when drilling holes in carbon fibre reinforced plastic composites, J. Mater. Process. Technol., Vol. 210,No. 1: pp. 1023-1034, 2019.

[7] Chen, W., Jiang, Q., Wang, Y., Zhang, Peridynamic analysis of drill-induced borehole damage, Engineering Failure Analysis, Vol. 104,No. 1: pp. 47-66, 2019.

[8] Pashmforoush, F., FarshbafZinati, R., Maleki, D., Investigation of ultrasonic vibration on thrust force, surface integrity, and geometrical tolerances during drilling of natural filler reinforced composites, Proceedings of the Institution of Mechanical Engineers, Part C: Journal of Mechanical Engineering Science. 2020.

[9] Pujana, J., Rivero, A., Celaya, A., Lopez, L., Analysis of ultrasonic-assisted drilling of Ti6Al4V, International Journal of Machine Tools & Manufacture, Vol. 49,No. 1: pp. 500-508, 2009.

[10] Chang, S.S.F., Bone, G.M., Burr height model for vibration assisted drilling of aluminum 6061-T6,Precision Engineering, Vol.34,No. 1: pp. 369-375, 2010.

[11] Yohei, N., Kazuhiro, O., Kenichiro, H., Junichi, K., Takeshi, W., Shinichi, M., Attempt to increase step feed by adding ultrasonic vibrations in micro deep drilling, Journal of Advanced Mechanical Design, Systems, and Manufacturing, Vol. 5,No. 1: pp. 129-138, 2011.

[12] Amini,S., Paktinat., H.,Barani, A. and Fadaei, Tehrani, A. Vibration Drilling of Al2024-T6, Materials and Manufacturing Processes, Vol. 28,No. 1: pp. 476–480, 2013.

[13] Barani, A., Amini, S.,Paktinat., H., Fadaei Tehrani, A., Built-up edge investigation in vibration drilling of Al2024-T6, Ultrasonics, Vol. 54,No. 1: pp.1300-1310, 2014

[14] Liu, D.F., Tang, Y. J. and Cong, W. L., A review of mechanical drilling for composite laminates, Composite Structures, Vol. 94,No. 1: pp. 1265-1279, 2012.

[15] Phadnis, V.A., Makhdum, F., Roy, A.,Silberschmidt, V.V., Experimental and numerical investigations in conventional and ultrasonically assisted drilling of CFRP laminate, 5th CIRP Conference on High Performance Cutting Procedia CIRP, 2012, London, pp. 455-459.

[16] Liu, J., Zhang, D.Y., Qin, L.g., Yan, L.S., Feasibility study of the rotary ultrasonic elliptical machining of carbon fiber reinforced plastics (CFRP). International Journal of Machine Tools & Manufacture,Vol. 53,No. 1: pp. 141-150, 2012.

[17] Krishnamorthy, A., Rajendra Boopathy, S., Palanikumar, K.,Davim, J.P.,Application of grey fuzzy logic for the optimization of drilling parameters for CFRP composites with multiple, performance characteristics, Measurement, Vol. 45,No. 1: pp. 1286-1296, 2012.

[18] Ding, K., Fu, Y., Su, H., Chen, Y., Yu, X., Ding, G., Experimental studies on drilling tool load and machining quality of C/SiC composites in rotary ultrasonic machining, Journal of Materials Processing Technology, Vol. 214,No. 1: pp. 2900-2907, 2014.

[19] Zou, F., Chen, J., An, Q., Cai, X. and Chen, M., Influences of clearance angle and point angle on drilling performance of 2D Cf/SiC composites using polycrystalline diamond tools, Ceramics International, 2019.

[20] Baraheni, M., Tabatabaeian, A., Amini, S. and Ghasemi, A.R. Parametric analysis of delamination in GFRP composite profiles by performing rotary ultrasonic drilling approach: Experimental and statistical study, Composites Part B, Vol. 172,No. 1: pp. 612–620, 2019.

[21] Sekaran, A. S. J., Kumar, K.P., Study on Drilling of Woven Sisal and Aloevera Natural Fibre Polymer Composite,Materials Today: Proceedings16, pp. 640-646, 2019.

[22] Wang, D., Onawumi, P.Y., Ismail, H. N., Dhakal, I. Popov, V.V. and Silberschmidt, A.R., Machinability of natural-fibre-reinforced polymer composites: Conventional vs ultrasonically-assisted machining, Composites Part A: Applied Science and Manufacturing, Vol. 119, No. 1: pp. 188-195, 2019.

[23] Soni, S. K., Thomas, B., Microstructure, Mechanical Properties and Machinability Studies of Al7075/SiC/h-BN Hybrid Nanocomposite Fabricated via Ultrasonic-assisted Squeeze Casting, FME Transactions, Vol. 48, No. 3: pp. 532-542, 2020.

[24] Elango, M., Annamalai, K., Machining Parameter Optimization of Al/SiC/Gr Hybrid Metal Matrix Composites using ANOVA and Grey Relational Analysis, FME Transactions, Vol. 48, No. 2: pp. 173-179, 2020.

[25] Waleed, W. A., Chathriyan, A., Sam Singh Vima, R., Experimental Investigation on the Influence of Process Parameters in Thermal Drilling of Metal Matrix Composites, FME Transactions, Vol. 46, No. 2: pp. 171-176, 2018.

[26] Zha, H., Feng, P., Zhang, D. Yu, Z. Wu, Material removal mechanism in rotary ultrasonic machining of high-volume fraction SiCp/Al composites,Int. J. Adv. Manuf. Technol., Vol. 97,No. 1: pp. 256-294, 2018.

[27] Kadivar, M. A., Yousefi, R., Akbari, J., Rahi, A., Nikoue, S.M., Burr Size Reduction in Drilling of Al/SiC Metal Matrix Composite by Ultrasonic Assistance, Advanced Materials Research, Vol. 410,No. 1: pp. 279-282, 2012.

[28] Kadivar, M.A.,Akbari, J., Yousefi, R.,Rahi, A., Nick, M.G.,Investigating the effects of vibration method on ultrasonic-assisted drilling of Al/SiCp metal matrix composites, Robotics and Computer-Integrated Manufacturing, Vol. 30, No. 3: pp. 344-350, 2014.

[29] Yang, H., Tian, S., Gao, T., Nie, J., You, Z., Liu, G., Wang, H. and Liu, X., High-temperature mechanical properties of 2024 Al matrix nanocomposite reinforced by TiC network architecture,Materials Science & Engineering A, Vol. 763,No. 1: pp. 125-136, 2019.

[30] Raj, S.O.N., Prabhu, S., Modeling and analysis of titanium alloy in wire-cut EDM using Grey relation coupled with principle component analysis, Australian Journal of Mechanical Engineering, Vol. 15,No. 1: pp. 198-209, 2016.

[31] Taskesen, A. and Kutukde, K., Experimental investigation and multi-objective analysis on drilling of boron carbide reinforced metal matrix composites using grey relational analysis, Measurement, Vol. 47,No. 1: pp. 321–330, 2013.

[32] Rajyalakshmi, G., Venkata Ramaiah, P., Multiple process parameter optimization of wire electrical discharge machining on Inconel 825 using Taguchi grey relational analysis, Int. J. Adv. Manuf. Technol., Vol. 69,No. 1: pp. 1249–1262, 2013.

[33] Khadir, A.I., Fathy, A., Enhanced strength and ductility of Al-SiC nanocomposites synthesized by accumulative roll bonding, Journal of Materials Research and Technology, In press, corrected proof, Available online 14 November 2019.

[34] Lahiri, S.K., Shaw, A., Ramachandra, L.S., On performance of different material models in predicting response of ceramics under high velocity impact, International Journal of Solids and Structures, Vol. 385,No. 1: pp. 96-107, 2019.

[35] Ucun, I., Aslantas, K.,Bedir, F., Finite element modeling of micro-milling: Numerical simulation and experimental validation, Machining Science and Technology, Vol. 20, No. 1: pp. 148-172, 2016.

[36] Ghasemi, A.H., Khorasani, A. and Gibson, I., Investigation on the Effect of a Pre-Center Drill Hole and Tool Material on Thrust Force, Surface Roughness, and Cylindricity in the Drilling of Al7075, Materials, Vol. 11,No. 1: pp. 1-14, 2018.

[37] Kavad, B.V., Pandey, A.B., Tadavi, M.V.,Jakharia, H.C., A Review Paper on Effects of Drilling on Glass Fiber Reinforced Plastic, Procedia Technology, Vol. 14,No. 1: pp. 457-464, 2014.

УЛТРАЗВУКОМ ПОТПОМОГНУТО БУШЕЊЕ ЛАМИНАТНОГ КОМПОЗИТА СА МАТРИЦОМ ОД АЛУМИНИЈУМА 2024 ОЈАЧАНОМ SiC НАНОЧЕСТИЦАМА

Ф. Пашмфоруш, Р.Ф. Зинати, А. Дадашзадех

Композити са матрицом од алуминијума имају широку примену у разним областима инжењерства због својих изузетних механичких својстава. Међутим, хетерогена структура ових материјала још увек представља изазов за ефикасну машинску обраду. Рад приказује експериментално истра-

живање перформанси обраде бушењем композитног материјала са матрицом од легуре алуминијума и бакра ојачаном SiC наночестицама, уз присуство ултразвучних вибрација. Утицај ултразвучних вибрација, тежинског удела SiC и параметара бушења је одређен помоћу кружне грешке и потисне силе бушења. Оптимизација параметара процеса је извршена коришћењем греј релационе анализе. Израчунавањем је утврђено да су оптимални параметри: ултразвучне вибрације, садржај SiC - 2 теж. %, брзина помоћног кретања – 20мм/мин, брзина вретена – 1400 рпм.